Macromolecules

Article

pubs.acs.org/Macromolecules

High Temperature Thermoplastic Elastomers Synthesized by Living Anionic Polymerization in Hydrocarbon Solvent at Room Temperature

Weiyu Wang,[†] Ralf Schlegel,[‡] Benjamin T. White,[†] Katherine Williams,[§] Dimitry Voyloy,[†,∥] Carlos A. Steren,[†] Andrew Goodwin,[†] E. Bryan Coughlin,[§] Samuel Gido,[§] Mario Beiner,[‡,#] Kunlun Hong,[⊥] Nam-Goo Kang,*[,†] and Jimmy Mays*[,†,∥]

[†]Department of Chemistry, University of Tennessee, Knoxville, Tennessee 37996, United States

[‡]Fraunhofer-Institut für Mikrostruktur von Werkstoffen und Systemen IMWS, Walter-Hülse-Str. 1, 06120 Halle (Saale), Germany

[§]Department of Polymer Science and Engineering, University of Massachusetts, Amherst, Massachusetts 01003, United States

[∥]Chemical Sciences Division and [⊥]Center for Nanophase Materials Sciences, Oak Ridge National Laboratory, Oak Ridge, Tennessee 37831, United States

[#]Naturwissenschaftliche Fakultät II, Martin-Luther-Universität Halle-Wittenberg, Heinrich-Damerow-Str. 4, 06120 Halle (Saale), Germany

Supporting Information

ABSTRACT: We present the synthesis and characterization of a new class of high temperature thermoplastic elastomers composed of polybenzofulvene−polyisoprene−polybenzofulvene (FIF) triblock copolymers. All copolymers were prepared by living anionic polymerization in benzene at room temperature. Homopolymerization and effects of additives on the glass transition temperature (T_g) of polybenzofulvene (PBF) were also investigated. Among all triblock copolymers studied, FIF with 14 vol % of PBF exhibited a maximum stress of 14.3 ± 1.3 MPa and strain at break of 1390 ± 66% from tensile tests. The stress−strain curves of FIF-10 and 14 were analyzed by a statistical molecular approach using a nonaffine tube model to estimate the thermoplastic elastomer behavior. Dynamic mechanical analysis showed that the softening temperature of PBF in FIF was 145 °C, much higher than that of thermoplastic elastomers with polystyrene hard blocks. Microphase separation of FIF triblock copolymers was observed by small-angle X-ray scattering, even though long-range order was not achieved under the annealing conditions employed. In addition, the microphase separation of the resulting triblock copolymers was examined by atomic force microscopy.

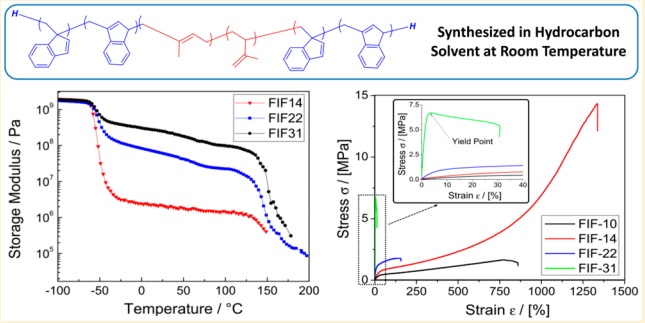

INTRODUCTION

Since its discovery and after thriving for 60 years, living anionic polymerization[1] has played a critical role in academic and industrial fields of polymer research because well-defined polymers with predictable molecular weight, narrow molecular weight distributions, and linear to complex macromolecular architectures can be prepared by this technique.[2,3] Additionally, living anionic polymerization can produce polymers with negligible impurities in quantitative yields and with short production times under industrially relevant conditions. Therefore, anionic polymerization remains more favorable for commercialization as compared to other controlled polymerization techniques.[4,5]

Styrenic thermoplastic elastomers (STPEs), prepared by living anionic polymerization in hydrocarbon solvents at mild temperatures, are largely used in the fields of paving, roofing, footwear, and medical tubing.[6] Such materials are A−B−A type triblock copolymers consisting of 1,4-polyisoprene (T_g ∼ −56 °C) or 1,4-polybutadiene (T_g ∼ −90 °C) as the rubbery B block which is physically cross-linked by glassy A blocks of polystyrene (PS, T_g ∼ 100 °C) on both ends. Triblock copolymers of polystyrene-*b*-polyisoprene-*b*-polystyrene (SIS), designed first by Milkovich and Holden,[7] were targeted to improve the green strength and hot tear properties of polyisoprene for production of synthetic rubber tires in large volume. However, this application failed, and other advanced consumptions of STPEs are still largely limited by the glass transition temperature of PS.[8] When the service temperature approaches 100 °C, softening of the PS domains weakens the

Received: December 4, 2015
Revised: February 29, 2016
Published: March 30, 2016

DOI: 10.1021/acs.macromol.5b02642
Macromolecules 2016, 49, 2646−2655

Table 1. Anionic Polymerization of BF in Benzene in the Absence of Additives

run	sample ID	BF (mmol)	initiator (mmol)	time (h)	M_n (kg/mol) calcd[a]	M_n (kg/mol) obsd[b]	PDI[c]	T_g[d] (°C)
1	PBF-5	3.92	0.111	0.5	4.5	4.8	1.16	127.0
2	PBF-10	1.56	0.0211	0.5	9.5	12.0	1.09	145.7
3	PBF-15	2.34	0.0203	0.5	14.8	14.6	1.08	147.5
4	PBF-20	3.90	0.0255	0.5	19.6	18.9	1.06	151.2
5	PBF-40	7.03	0.0235	1	38.3	42.3	1.08	152.2
6	PBF-60	8.59	0.0183	2	60.1	60.6	1.12	153.4
7	PBF-80	10.16	0.0163	2	79.8	86.4	1.11	153.1
8	PBF-200	16.41	0.0105	6	200	175	1.45[e]	163.5

[a] M_n(calcd) = (MW monomer) × [BF]/[initiator]. [b] M_n(Obsd) was characterized by SEC equipped with triple detectors: refractive index (RI), light scattering (LS) and viscometer detectors. [c] PDI was calculated by SEC with polystyrene standard in THF. [d] T_g was measured by DSC on the second heating scans. [e] Bimodal.

physical cross-linking, leading to a sharp drop in tensile strength.

In order to improve the upper service temperature (UST) of TPEs, incorporating a glassy block with glass transition temperature higher than 100 °C is important. High T_g polymers such as poly(α-methylstyrene) (T_g ~ 173 °C)[9] or poly(α-methyl-*p*-methylstyrene) (T_g ~ 183 °C)[10] could be used as an alternative glassy block to replace PS. However, the bulkiness introduced by the methyl group at the α position leads to low ceiling temperatures (<6 °C), requiring low polymerization temperatures (−78 °C) in polar solvents such as tetrahydrofuran (THF) in order to achieve quantitative yields. Use of PS derivatives with bulky pendent group at the para position, such as poly(*tert*-butylstyrene) (PtBS, T_g ~ 130 °C)[11] or poly(*p*-adamantylstyrene) (P-AdmS, T_g ~ 203 °C),[12] could also increase the UST of TPEs. However, the liphophilic nature introduced by these pendent groups causes phase blending with polydienes and reduces tensile strength. Catalytic hydrogenation to fully saturate PS into poly(vinylcyclohexane) (PVCH, T_g ~ 147 °C)[13,14] produces TPEs with higher UST and better thermal stabilities, but these conditions will hydrogenate polydienes at the same time. The additional cost as well as the complete hydrogenation has limited the development of this approach, especially in applications where unsaturated polydienes are required.

As another approach, anionic polymerization of methyl methacrylate[15,16] and other methacrylates[17,18] in THF at −78 °C was performed by initiating methacrylate monomer from a difunctional polydiene anion. Since polymerization of butadiene or isoprene in polar solvents will form less of the desired 1,4 microstructure, and thus dramatically increase the T_g, the difunctional polydiene anion needs to be synthesized in a hydrocarbon solvent. Because of the low polymerization temperature and high cost, this approach is not suitable for large scale industrial application. The various TPEs synthesized by other living/controlled polymerization techniques have also shown limited industrial applications. The use of cationic polymerization to produce high T_g polymers[19−23] suffers from the same limitation due to the polymerization temperature. On the other hand, high service temperature TPEs prepared by controlled radical polymerization such as atom transfer radical polymerization require longer reaction times and pretermination to control the polymerization and generally contain metal catalyst.[24,25]

Benzofulvene (BF) is a conjugated diene hydrocarbon monomer that undergoes polymerization by anionic, cationic, and radical mechanisms.[26−28] As a derivative of fulvene,[29] BF displays living anionic polymerization behavior in both THF as a polar solvent and benzene as a hydrocarbon solvent. The microstructure of the resulting polybenzofulvene (PBF) depends on the polymerization solvents, temperatures, additives, and initiators. Regardless of the microstructure, for PBF with a molecular weight above 10 kg/mol, the glass transition temperature is higher than 140 °C.[28] The high glass transition temperature along with the capacity to undergo living anionic polymerization in hydrocarbon solvents makes BF an ideal candidate as the glassy building block for developing thermoplastic elastomers with higher upper service temperature.

In this study, we present the synthesis and characterization of A−B−A triblock copolymer type thermoplastic elastomers, with polyisoprene as the elastic B block and PBF as the glassy A block, via anionic polymerization. FIF triblock copolymers with four different compositions were prepared by living anionic polymerization in benzene at room temperature. The tensile testing of FIF samples was carried out to obtain stress−strain curves, and their mechanical properties are compared with those of Kraton D1112P SIS.[30,31] Based on tensile testing, the optimal chemical composition of FIF for use as a TPE was investigated. Small-angle X-ray scattering (SAXS) were used to confirm the microphase separation between PI and PBF. Atomic force microscopy (AFM) was employed to examine the morphology of FIF copolymer. The effect of polar additives on the T_g of PBF is also presented.

EXPERIMENTAL SECTION

Materials. Isoprene (Fisher, >99%), *n*-BuLi (Fisher, 2.5 M in hexanes), 2-chlorobutane (Fisher, >99%), hexane (Fisher, >99.5%), methanol (Fisher, ≥99.9), benzene (Aldrich, ≥99.9), cyclohexane (Fisher, >99%), and 2-butanol (Aldrich, >99%) were purified according to high vacuum techniques reported previously.[32] *sec*-BuLi was prepared by reacting 2-chlorobutane with Li metal under vacuum. 1,2-Dimethoxyethane (DME, Aldrich, >99.9%) was distilled over CaH_2, potassium dispersion two times, and diluted with anhydrous benzene. 1,4-Diazabicyclo[2.2.2]octane (DABCO, Aldrich, >99%) was sublimated three times under high vacuum and diluted with anhydrous benzene. Tetramethylethylenediamine (TMEDA, Aldrich, ≥99%) was distilled over CaH_2, potassium/sodium alloy, and diluted with cyclohexane. Lithium (Aldrich, >99%, granular), sodium (Aldrich, >99.9%, cubes), potassium (Aldrich, >98%, chunks), indene (TCI, 95%), paraformaldehyde (Aldrich, 95%, powder), potassium *tert*-butoxide (TCI, 1.0 M in tetrahydrofuran), ethylmagnesium bromide (Aldrich, 3.0 M in diethyl ether), 1,3-bis(1-phenylvinyl)benzene (PEB, donated by Dow Chemical, >95%), butylated hydroxytoluene (BHT, Aldrich, >99%), and IRGANOX B 225 (BASF) were used as received. The solution of *sec*-BuLi and *sec*-BuOLi in hexane and the solution of

DOI: 10.1021/acs.macromol.5b02642
Macromolecules 2016, 49, 2646−2655

Table 2. Anionic Polymerization of BF in Benzene in the Presence of Additives

run	sample ID	BF (mmol)	initiator (mmol)	[additive]/[initiator]	M_n (kg/mol) calcd[a]	M_n (kg/mol) obsd[b]	PDI[c]	yield (%)	T_g[d] (°C)
9	PBF_DME_16	1.54	0.0121	10	16.3	15.9	1.10	99	191.5
10	PBF_DME_40	3.08	0.0099	10	40.0	39.0	1.12	98	198.7
11	PBF_DABCO_20	3.18	0.0201	3	20.3	28.5	1.86[e]	98	187.0
12	PBF_TMEDA_20	3.40	0.0220	1	19.8	12.2	2.35[e]	12	155.2
13	PBF_*sec*-BuOLi_7	3.16	0.0554	10	7.3	6.9	1.16	99	142.3
14	PBF_*sec*-BuOLi_23	4.05	0.0228	10	22.7	23.1	1.10	99	153.1

[a] M_n(calcd) = (MW monomer) × [BF]/[initiator]. [b] M_n(obsd) was characterized by SEC equipped with triple detectors: refractive index (RI), light scattering (LS), and viscometer detectors; dn/dc of PBF was 0.227. [c] PDI was calculated by SEC with polystyrene standard in THF. [d] T_g was measured by DSC on the second heating scans. [e] Multimodal. Initiator: *n*-BuLi (runs 9,10) and *s*-BuLi (runs 11−14).

(1,3-phenylene)bis(3-methyl-1-phenylpentylidene) dilithium initiator in benzene were prepared according to reported procedure and diluted into desired concentration.[32] Generally, the solution of DLI in benzene was prepared by addition of 2.2 equiv of *sec*-BuLi (27.06 mmol) into 1,3-bis(1-phenylvinyl)benzene (12.3 mmol, 3.47g) in hexane (300 mL). Since DLI is insoluble in hexane, as the reaction proceeded DLI was precipitated inside the reactor. After removing hexane by filtration, the resulting red solid was diluted with benzene and calibrated by conducting a polymerization with isoprene and measuring the molecular weight of the resulting polymer. BF monomer was synthesized based on the literature,[26] diluted with anhydrous benzene (0.3−0.5 M), and ampulized under high vacuum condition. All ampules of monomer, initiator, and additives were stored at −30 °C.

Anionic Polymerization of BF Monomer. All anionic polymerizations were carried out under high vacuum condition (10^{-6} Torr) with purged all glass apparatus equipped with break-seals. In a typical polymerization, the solution of BF (7.03 mmol, 0.900 g) in benzene was introduced into the solution of *sec*-BuLi (0.0235 mmol) in hexane, and the solution of polymer was quenched with degassed methanol after 1 h. All polymers were precipitated into large excess of methonal with 0.5% BHT, filtered, and dried. The characterization of PBF was performed by ^{1}H NMR, size exclusion chromatography (SEC), and differential scanning calorimetry (DSC). The yield of PBF was quantitative (42.3 kg/mol, yield = 100%, molecular weight distribution PDI = 1.08, T_g = 152.2 °C, Table 1, run 5).

Anionic Polymerization of BF Monomer in the Presence of Additives. The solution of DME (0.121 mmol) in benzene was introduced into the solution of *n*-BuLi (0.0121 mmol) in hexane at 0 °C using an ice bath and kept at 5 °C. The solution of BF (1.54 mmol, 0.197 g) in benzene was added to the initiation system. After complete polymerization over 1 h, the solution of polymer was quenched with degassed methanol, and the purification was performed as described above. The yield of PBF was 99% (16.3 kg/mol, PDI = 1.10, T_g = 191.5 °C, Table 2, run 9). For anionic polymerizations of BF monomer in the presence of other additives, similar addition and purification procedures were employed. When *sec*-BuOLi was used as the additive, the polymerization was carried out at room temperature.

Triblock Copolymerization of Isoprene and BF. In a typical polymerization procedure, DLI and *sec*-BuOLi were first mixed in benzene followed by addition of isoprene. After complete consumption of isoprene, as monitored by SEC over 5 days, BF monomer (5.75 mmol, 0.737 g) was introduced into the solution of living polyisoprene (0.0614 mmol, 4.36 g) in benzene, and the resulting solution of this triblock copolymer was terminated with degassed methanol after 8 h. All FIF triblock copolymers were precipitated into large excess of methanol with 0.5 wt % of IRGANOX B 225 as the long-term thermal stabilizer. Precipitates were filtered and dried in vacuum oven for 48 h.

Preparation of Samples. For tensile tests, a solution of 2 g of polymer in 80 mL of toluene was stirred overnight at room temperature and casted into a glass bowl with inner diameter of about 90 mm and evaporated slowly over 7 days. Upon removing residual solvent from the films, all samples were annealed at 70 °C under vacuum (10^{-1} Torr) and stamped into dog bone shaped specimens (type 5A, ISO 527/2) with film thickness around 0.2−0.3 mm. For dynamic mechanical analysis, polymer solutions were cast into smaller PTFE dishes, resulting in film thicknesses of 0.5−0.6 mm. For the measurement of small-angle X-ray scattering, we first attempted to anneal solvent cast samples at 170 °C for 24 h under N_2 in order to achieve a thermodynamically equilibrated morphology. However, all samples of PI and PBF were thermally cross-linked as evidenced by SEC traces. Thus, all samples were annealed at 155 °C for 12 h under dynamic vacuum. No noticeable cross-linked polymers with very high molecular weights were detected by SEC. For atomic force microscopy, mold pressed polymer sheet was trimmed and microtomed at −120 °C using a diamond knife into ultrathin section with thickness around 100 nm.

Measurements. ^{1}H and ^{13}C NMR were measured on a Varian Mercury 500 instrument using deuterated chloroform ($CDCl_3$) for homopolymers of PBF and using deuterated tetrahydrofuran (THF-d_8) for PBF-*b*-PI-*b*-PBF (FIF). Molecular weight and molecular weight distribution were measured by size exclusion chromatography in THF at 40 °C with flow rate of 1.0 mL/min using a Polymer Laboratories GPC-120 SEC equipped with four detectors of a Polymer Laboratories refractometer, a Precision Detector PD2040 (two angle static light scattering detector), a Precision Detector PD2000DLS (dynamic light scattering detector), and Viscotek 220 differential viscometer. The column set installed is the Polymer Laboratories PLgel; 7.5 × 300 mm; 10 μm; 500, 1 × 10^4, 1 × 10^6, and 1 × 10^7 Å. Glass transition temperatures were measured by a TA Instruments Q-2000 differential scanning calorimeter (DSC) from −80 to 200 °C at a heating rate of 10 °C/min with a 5 min isothermal hold at the maximum and minimum temperatures. Reported glass transition temperatures were based on the second heating scans. Thermal stability was examined using a TA Instruments Q-50 TGA. A 5−10 mg sample was placed on platinum pan and equilibrated at 30 °C. The temperature was ramped from 30 to 800 °C at a rate of 10 °C/min under a nitrogen atmosphere. Tensile tests were performed with a Zwick/Roell Z050 at the cross-head speed of 15 mm/min, clamping distance of 50 mm, and measuring distance of 15 mm. A multiXtens extensometer was applied to obtain the displacement. For each polymer sample three tensile specimens were tested. Dynamic mechanical analysis measurements were performed with an ARES rheometer in torsion mode with a testing frequency of 10 rad/s and a strain amplitude of 0.2%. The temperature was increased in steps of 3 K with 60 s equilibration time after each step. Small-angle X-ray scattering profiles were obtained from a Rigaku S-Max 3000 using Ni-filtered Cu Kα radiation (wavelength is 1.54 Å) operated at 40 kV, 200 mA with pinholes collimation system located 87.52 cm from the sample. AFM measurements were performed on a Nanowizard II (JPK Instruments, Berlin, Germany) scanning probe microscope using super sharp silicon tips. The images were obtained by operating the instrument in the tapping mode at room temperature. Ultrathin sections (100 nm) were trimmed from a mold-pressed sheet with a cryo-ultramicrotome (PT-PC Powertome with CR-X cryo unit) at a temperature of −120 °C using a diamond knife.

DOI: 10.1021/acs.macromol.5b02642
Macromolecules 2016, 49, 2646−2655

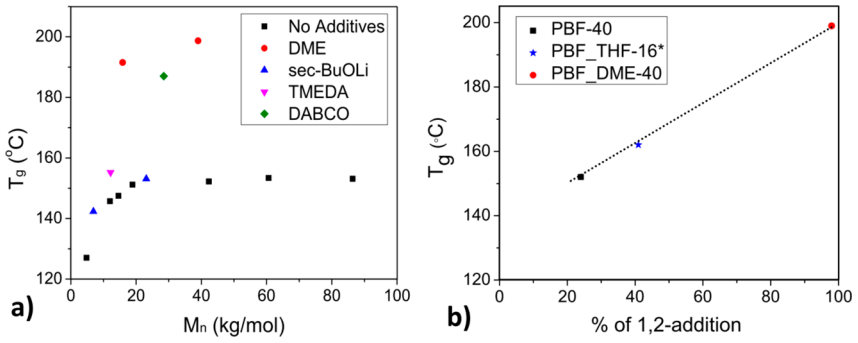

Figure 1. (a) T_g versus M_n of PBF synthesized with different additives: DME (red cycle), *sec*-BuOLi (blue triangle), TMEDA (pink triangle), DABCO (green square), and no additives (black square). (b). Plot of percentage of 1,2-microstructure versus T_g. *Data for PBF_THF-16 was taken from Table 1, run 3, in ref 28.

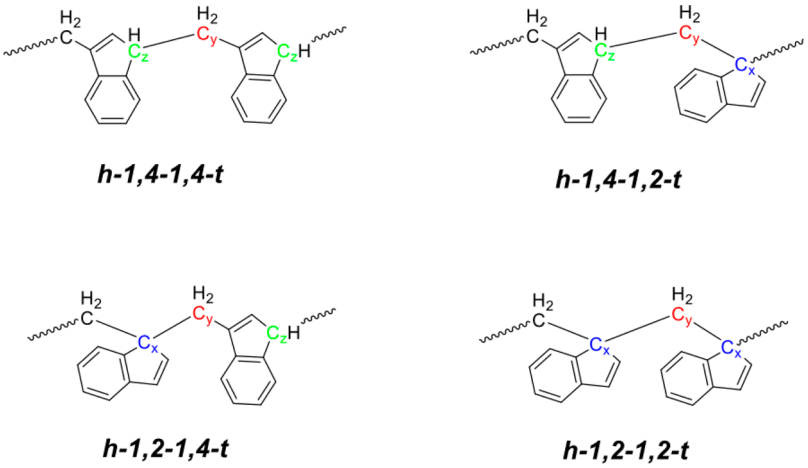

Figure 2. Possible dimers of PBF.[26,27]

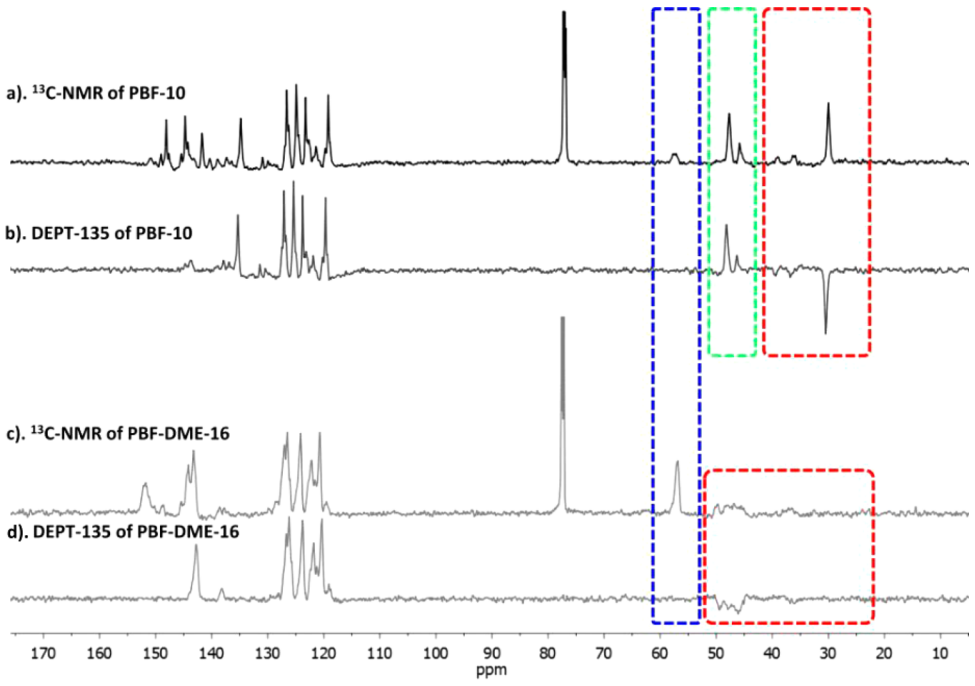

Figure 3. ^{13}C NMR of PBF: (a) ^{13}C NMR of PBF-10, (b) DEPT-135 of PBF-10, (c) ^{13}C NMR of PBF-DME-16, and (d) DEPT-135 of PBF-DME-16.

Modeling of Tensile Data. To understand the deformation behavior of block copolymers on molecular scale, the nonaffine and non-Gaussian tube model was adapted and applied to the stress−strain data of FIF copolymers. The model quantifies the amount of the

DOI: 10.1021/acs.macromol.5b02642
Macromolecules 2016, 49, 2646−2655

Scheme 1. DLI Approach To Synthesize FIF Triblock Copolymer

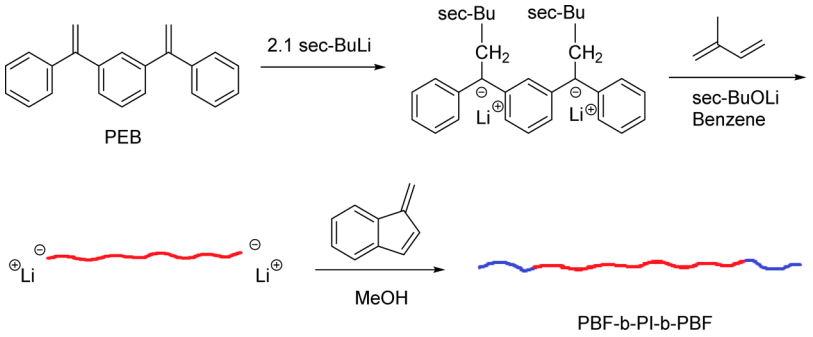

Table 3. Composition of FIF Triblock Copolymers

		PI (kg/mol)		FIF (kg/mol)		PBF (kg/mol)	φ_{PBF} (%)	
run	sample ID	M_n [a]	PDI [b]	M_n [a]	PDI [b]	M_n [c]	NMR	SEC
15	FIF-10	76.7	1.08	87.8	1.08	5.6	9.5	10.1
16	FIF-22	76.7	1.08	98.2	1.10	10.7	22.0	19.1
17	FIF-31	76.7	1.08	106.0	1.09	20.0	30.9	30.1
18	FIF-14	87.6	1.11	110.6	1.14	11.5	13.6	12.8

[a] M_n of PI and FIF was characterized by SEC equipped with triple detectors: refractive index (RI), light scattering (LS), and viscometer detectors. [b] PDI was calculated from SEC with polystyrene standard in THF. [c] M_n of PBF was calculated from $(M_{n,FIF} - M_{n,PI})/2$.

"chemical" (G_c) and the "physical" (entanglements, G_e) part of the overall modulus. Further, information is obtained on the average number of statistical segments between two successively trapped entanglements.[33,34] In contrast to chemically cross-linked elastomers, the application of a rubber elasticity model requires additional explanations when used for tensile data of TPEs. In TPEs, the glassy domains act as cross-links, but they are of physical nature. On one hand, these domains can be considered as dissolvable cross-links, and, on the other hand, they introduce filler like characteristics such as strain and stress amplification, expressed in terms of an amplification factor f.[34] Based on theoretical results, a Padè approximation with

$$f = 1 + 2.5\phi/(1 - 2\phi) \quad (1)$$

is given as a reasonable choice for a filler volume fraction of $\phi \sim 0.35$.[34] Amplification usually accounts for both stress and strain.[35] For simplification, we will limit our considerations to stress amplification only. This results in $\sigma(\lambda) = f\sigma_0(\lambda)$, where $\sigma_0(\lambda)$ is the stress response of the "unfilled" material. For the stress response of the elastomer matrix the nonaffine and non-Gaussian tube model in eq 2 is applied.[33,34]

$$\sigma_0(\lambda) = G_c\left(\lambda - \frac{1}{\lambda^2}\right)\left(\frac{1 - T_e/n_e}{\left(1 - T_e/n_e\left(\lambda^2 + \frac{2}{\lambda} - 3\right)\right)^2} - \frac{T_e/n_e}{1 - T_e/n_e\left(\lambda^2 + \frac{2}{\lambda} - 3\right)}\right) + 2G_e\left(\frac{1}{\sqrt{\lambda}} - \frac{1}{\lambda^2}\right) \quad (2)$$

Equation 2 holds for uniaxial deformation taking into account an incompressible elastomer matrix. It contains three parameters: the chemical and the physical cross-link modulus (G_c, G_e) and the parameter $n = n_e/T_e$. The latter represents the number of statistical segments between two successively trapped entanglements with the trapping factor T_e. The model curve of eq 2 can be subdivide into three regions: the neo-Hookean, the Gaussian region (approximately constant slope), and the upturn region. While n controls the upturn region, the impact of G_c and G_e becomes most obvious in the Gaussian region, where G_c corresponds to the slope. Changes in G_e result in a vertical shift.

RESULTS AND DISCUSSION

Anionic Polymerization of BF in Benzene at Room Temperature without Polar Additive. Previously, Ishizone examined the anionic polymerization of BF in benzene at 0, 40, and 55 °C.[27] The molecular weight was targeted from 2.8 to 29 kg/mol. In order to fully examine the anionic polymerization behavior of BF, especially at room temperature, we first polymerized benzofulvene in benzene with *sec*-BuLi as initiator with targeted molecular weight ranging from 4.5 to 200 kg/mol (Table 1). Controlled molecular weights and narrow polydispersity indexes (PDI < 1.16) were achieved when the target molecular weight was lower than 86.4 kg/mol (Table 1, runs 1−7; see Figure S1 for SEC curves in Supporting Information). All polymers were recovered in quantitative yield. However, the polymerization of BF targeting 200 kg/mol, as shown in Table 1, run 8, was uncontrolled and exhibited a bimodal distribution with a M_n of 175 kg/mol lower than calculation. The glass transition temperature of PBF increased from 127 to 153 °C as the M_n was increased from 4.5 to 86.4 kg/mol (black squares in Figure 1). Slightly change of T_g was observed after the molecular weight was above 18.9 kg/mol. Quantitative ^{13}C NMR analysis indicated 22%−28% of 1,2-microstructure was presented in PBF synthesized with *sec*-BuLi

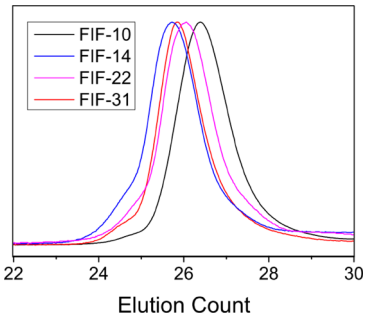

Figure 4. SEC curves of FIF triblock copolymers.

DOI: 10.1021/acs.macromol.5b02642
Macromolecules 2016, 49, 2646−2655

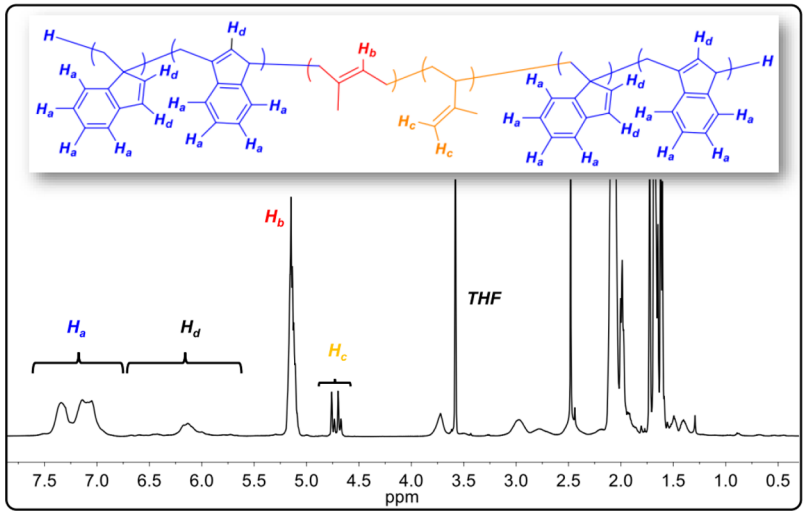

Figure 5. ^{1}H NMR of FIF-22 measured in THF-d_8.

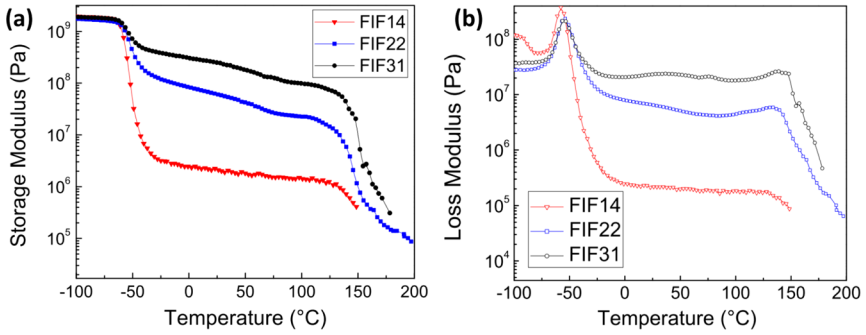

Figure 6. DMA of FIF triblock copolymers: (a) storage modulus vs temperature and (b) loss modulus vs temperature.

Table 4. Mechanical Property Parameters of FIF

	tensile test			nonaffine tube model			
sample ID	E (MPa)	σ_M (MPa)	ε_B (%)	G_c (kPa)	G_e (kPa)	n	fit range
FIF-10	2.8 ± 0.2	1.9 ± 0.3	855 ± 143	126 ± 3	256 ± 19	682 ± 57	1–7.8
FIF-14	2.6 ± 0.2	14.3 ± 1.3	1394 ± 66	191 ± 20	349 ± 11	352 ± 8	1–11
FIF-22	16.4 ± 0.4	1.5 ± 0.03	160 ± 28				
FIF-31	246 ± 11.5	5.3 ± 0.03	31 ± 3				

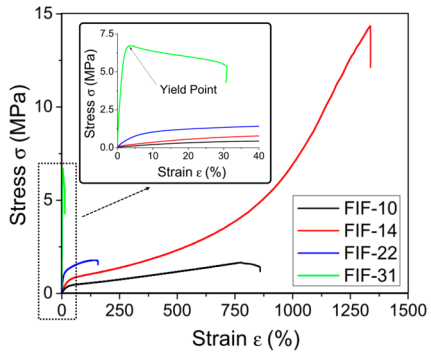

Figure 7. Stress–strain curve of FIF triblock copolymers.

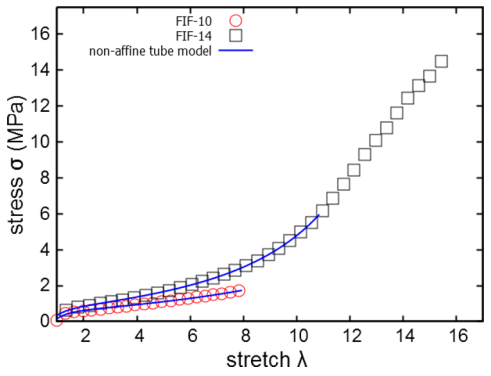

Figure 8. Nonaffine tube model analysis of FIF triblock copolymers.

without polar additive. This observation is consistent with previously reported data where the molecular weight was targeted from 2.8 to 29 kg/mol.[28]

Effects of Additives on Glass Transition Temperature. One feature of anionic polymerization of diene monomers is that different polar additives can change the reactivity of the propagating anion and lead to polymers with different microstructures, i.e., tunable 1,2- and 1,4-addition.[36] Different from "conventional additives" which are small molecules added to compound during processing, the terminology "additives" as

DOI: 10.1021/acs.macromol.5b02642
Macromolecules 2016, 49, 2646–2655

Table 5. SAXS Measurement of FIF Triblock Copolymers

sample	q^* (nm^{-1})	$d_{AV,PBF,sph}$ (±0.5 nm)	$d_{AV,\ PBF-PI}$
FIF-10	0.178	35.3	16.1
FIF-14	0.171	36.7	18.8
FIF-22	0.140	44.9	
FIF-31	0.110	57.1	

used in this paper indicates chemicals added during the polymerization to change the microstructure of resulting polymers. Generally, glass transition temperatures (T_g) of polydienes such as polybutadiene and polyisoprene increase as the percentage of 1,2-addition is increased relative to that of 1,4-addition in the polymer chain. Ishizone studied anionic polymerization of BF with different solvents, temperatures, and initiators.[28] Attempts to tailor the microstructure of PBF by using polar additives in hydrocarbon solvent was not reported in their work. Thus, it is of our interest to investigate the effects of polar additives on the microstructure and the glass transition temperature of PBF.

Different from isoprene or butadiene, BF is a relative bulky monomer similar to 1,3-cyclohexadiene (CHD). For the anionic polymerization of CHD, controlled polymerization behavior was observed when additives such as 1,4-diazabicyclo[2.2.2]octane (DABCO), dimethoxyethane (DME), and *N,N,N′,N′*-tetramethylethylenediamine (TEMDA) were used during the polymerization in benzene or cyclohexane. The percentage of 1,2-addition in the resulting poly(1,3-cyclohexadiene) (PCHD) was 7%, 28%, and 45% with respect to these three additives. The glass transition temperature increased as the percentage of 1,2-addition increased.[37,38] Thus, the same initiation systems used in tailing microstructure of PCHD were employed in this research.

Surprisingly, when DME was used as the additive, the resulting polymers displayed glass transition temperatures above 190 °C (red cycle in Figure 1a). The PBF_DME_40 (Table 2, run 10) with M_n of 39.0 kg/mol exhibited higher T_g of 198.7 °C than 191.5 °C of PBF_DME_16 (Table 2, run 9) with M_n of 15.9 kg/mol. Both polymerizations yielded polymers having predicted M_n, narrow polydispersity indexes (PDI < 1.12) and with quantitative yield. ^{13}C NMR spectra showed that PBF_DME_16 has about 99% of 1,2-addition microstructure. The high T_g feature of PBF_DME is attributed to the high percentage of 1,2-microstructure in the polymer chain. It is worth noting that polymerizations with DME as the additive were performed at 5 °C with *n*-BuLi as the initiator. In hydrocarbon solvent, lower polymerization temperature of diene monomer leads to higher percentage of 1,2-addition.[39]

Unlike controlled polymerization of CHD, polymerizations of BF using either 1,4-diazabicyclo[2.2.2]octane (DABCO) or tetramethylethylenediamine (TEMDA) as additives were uncontrolled, where broad MWDs and multimodal curves were observed in SEC. 12% and 86% yields were obtained using the TEMDA and DABCO initiation systems, respectively. The PBF_DABCO_20 (Table 2, run 11) synthesized with DABCO as additive showed high T_g of 187 °C (green square in Figure 1a), however, with a yield of 86%. It has been observed that the living polymer anion has relatively low stability in the presence of DABCO after the the consumption of monomers.[40,41] This might be the reason we observed low yields and uncontrolled polymerization of benzofulvene with DABCO as the additive.

Polymerization of BF with TMEDA was also uncontrolled with a yield of only 12% (PBF_TMEDA_20, run 12, Table 2). The low yield and uncontrolled polymerization are likely due to lithiation between benzene and the *sec*-BuLi/TMEDA complex.[42] Generally cyclohexane is employed as the hydrocarbon solvent when TMEDA is used as the additive during anionic polymerization. However, PBF has very limited solubility in cyclohexane. Thus, we proceeded to carry out the polymerization in benzene in order to evaluate the glass transition temperature of the polymer. The resulting polymer PBF_TMEDA_20 showed a T_g of 155.2 °C (pink triangle in Figure 1a), similar to the T_g of PBF synthesized without additive.

Additional to the three aforementioned additives, we also evaluated the polymerization behavior of benzofulvene with *sec*-BuOLi (lithium *sec*-butoxide) as the additive since this additive is critical to preparation and use of the difunctional living polyisoprene anion.[43] PBF prepared by using *sec*-BuOLi showed lower T_g of 142.3 and 153.1 °C (blue triangle in Figure 1a) with 22% and 28% of 1,2-addition, respectively (runs 13 and 14 in Table 2), which is similar to polymerization without any additives. Both polymerizations produced polymers with predicted M_n, narrow PDI and quantitative yield. For the anionic polymerization of isoprene and butadiene, it has been observed that *sec*-BuOLi has little effect on polydiene microstructure and T_g giving products comparable to those obtained without any additives.[43]

Finally, we plot T_g versus percentage of 1,2-addition where molecular weight is sufficiently high that T_g does not depend on M_w (Figure 1b). The data we used are PBF-40 (black square in Figure 1b, M_n = 38.3 kg/mol, T_g = 152 °C with 24% of 1,2-microstructure), PBF_DME-40 (red cycle in Figure 1b, M_n = 40.0 kg/mol, T_g = 199 °C with 98% of 1,2-microstructure), and PBF_THF-16 (blue star in Figure 1b). The glass transition temperature (T_g = 162 °C) and molecular weight (M_n = 16 kg/mol) of PBF_THF-16 were reported in a previous publication

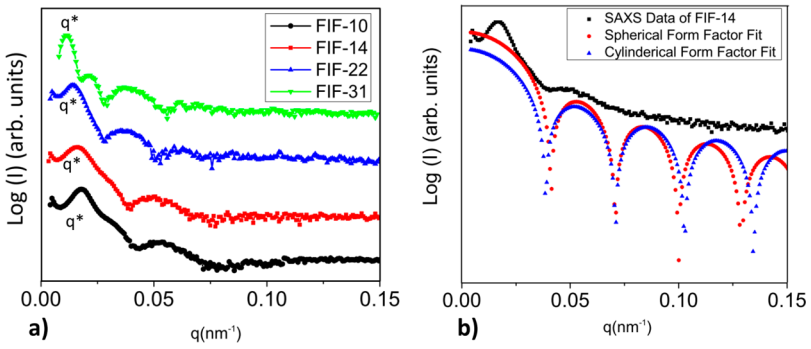

Figure 9. SAXS data for FIF triblock copolymers: (a) SAXS profile of FIF triblock copolymers; (b) SAXS data fitting of FIF-14.

DOI: 10.1021/acs.macromol.5b02642
Macromolecules 2016, 49, 2646−2655

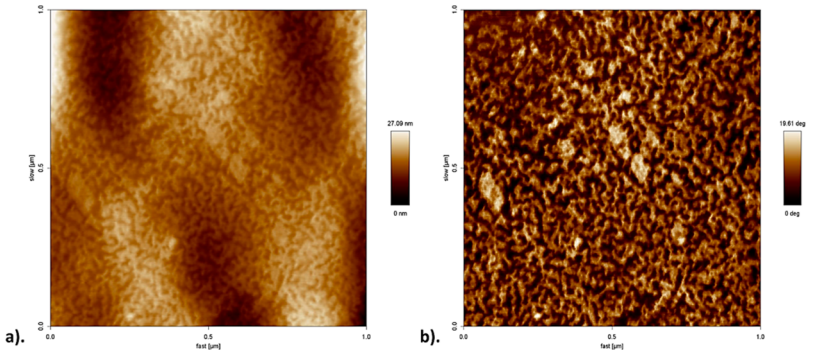

Figure 10. AFM of FIF-10: (a) height image; (b) phase image.

by Ishizone (Table 1, run 3).[28] As the percentage of 1,2-addition increased from 24 to 41 to 98%, the glass transition temperature increased linearly from 152 to 162 to 199 °C.

Microstructure Analysis of PBF Synthesized without Additive and with DME as the Additive. In order to analyze the microstructure of PBF, we tracked chemical shifts of three different carbons: C_x for quaternary carbon in 1,2-addition, C_y for methylene carbon in between 1,2- and 1,4-addition, and C_z for tertiary carbon of 1,4-addition. According to previous reports,[26,27] there are four possible dimers in polybenzofulvene if stereoregularity is not taken into consideration: h-1,4−1,4-t; h-1,4−1,2-t; h-1,2−1,4-t, and h-1,2−1,2-t. Here, h means head and t means tail in the structure (Figure 2). In Figure 3, the signal at 57 ppm was assigned to C_x in both PBF-10 and PBF-DME-16 since this signal was only observed in ^{13}C NMR spectra. Signals at 46 and 48 ppm for PBF-10 (spectra a and b in Figure 3) were assigned to C_z since these signals were observed in both ^{13}C NMR spectra and positive phase in DEPT-135. Integration from quantitative ^{13}C NMR spectra of C_x and C_z showed 26% of 1,2-addition in PBF-10. Surprisingly, the C_z signal was not observed in PBF-DME-16 and only C_y signal was observed from 25 to 50 ppm. Thus, the microstructure in PBF-DME-16 was dominated by 1,2-addition. Signals in ^1H NMR spectra in Figure S2 (see Supporting Information) were rather broad and could not be used to analyze the microstructure.

Triblock Copolymerization of BF with Isoprene. There are three possible methods to prepare polybenzofulvene−polyisoprene−polybenzofulvene (FIF) triblock copolymers by living anionic polymerization. The first method is to sequentially initiate BF, isoprene, and BF monomer after complete consumption of the previous monomer (sequential anionic polymerization). The second methods is to couple living polybenzofulvene−polyisoprene diblock copolymer through the polyisoprene chain end anion using a difunctional linking agent such as dichlorodimethylsilane or α,α′-dibromo-*p*-xylene (anion coupling reaction). The third method is to initiate BF polymerization using a difunctional living polyisoprene anion prepared by a difunctional lithium initiator (difunctional initiator method). Since isoprene cannot be initiated by polybenzofulvene anion,[27] neither sequential anionic polymerization using BF monomer as first monomer nor anion coupling reaction using polybenzofulvene−polyisoprenyllithium anion could be used to prepare polybenzofulvene-*b*-polyisoprene-*b*-polybenzofulvene (FIF) triblock copolymers. To synthesize FIF triblock copolymers with four different compositions (Scheme 1), the third approach involving the use of a difunctional lithium initiator (DLI)/*sec*-BuOLi (molar ratio = 10), prepared in benzene at room temperature, was employed. FIF with 9.5 vol % (FIF-10), 13.6 vol % (FIF-14), 22.0 vol % (FIF-22), and 30.9 vol % (FIF-31) PBF were prepared by the DLI approach (Table 3). In FIF-10, -22, and -31 (runs 15−17), the M_n of PI is 76.6 kg/mol, whereas FIF-14 (run 18) has 87.6 kg/mol of PI M_n. All resulting triblock copolymers have narrow PDIs and predicted molecular weight, which were confirmed by SEC (Figure 4) and ^1H NMR (Figure 5). As shown in Figure 5, signals of 6.75−7.60 ppm, 4.95−5.25 ppm, and 4.55−4.80 ppm in the ^1H NMR spectra correspond to aromatic proton (H_a) in PBF block, 1,4-addition proton (H_b) in PI block, and 3,4-addition proton (H_c) in PI block, respectively. According to the analysis of ^1H NMR spectra, we confirmed that PI block in FIF triblock copolymers has 93% 1,4-addition. The volume percentage of PBF presented in FIF was calculated based on integration ^1H NMR with the density of PBF homopolymers of 1.146 g/cm^3 as well as on SEC as listed in Table 3. The thermal properties of FIF were evaluated using DSC and TGA as shown in Figures S3 and S4 (see Supporting Information).

Dynamic Mechanical Analysis (DMA). The relaxation behavior of the triblock copolymers FIF-14, -22, and -31 was investigated by dynamic shear measurements. Temperature sweeps measured in the range from −100 to 200 °C at a frequency of 10 rad/s are shown in Figure 6. A low temperature relaxation process was observed at −54 °C corresponding to the glass-to-rubber transition (α_{PI}) of the PI phase indicated by a stepwise decrease in $G'(T)$ and a peak in $G''(T)$. The observed softening temperature was close to the thermal glass temperature T_g = −56.7 °C of PI as taken from DSC scans with a rate of 10 °C/min (Figure S3). During further heating the storage modulus $G'(T)$ showed another pronounced drop when the temperature approaches 140 °C. This drop in $G'(T)$ can be related to the glass-to-rubber transition of the PBF hard phase (α_{PBF}) and was accompanied by a broad peak in the loss modulus $G''(T)$. The measured softening temperatures were consistent with the T_g values of the PBF end block reported in Table 1. The storage modulus $G'(T)$ in the temperature range between the α_{PI} and α_{PBF} processes increased systematically as the volume fraction of PBF was increased. Low G' values of a few MPa were obtained in this temperature range for FIF-14 similar to the situation in classical TPEs, and filled elastomers while much larger storage moduli (30 MPa < G' < 300 MPa) were found for FIF-22 and FIF-31. This indicates a transition from isolated PBF domains in FIF-14 to a percolated PBF phase in FIF-22 and FIF-31. Note that a certain temperature-dependent decrease in G' occurs for all samples in the range between the α- relaxations of both phases, α_{PI} and α_{PBF},

DOI: 10.1021/acs.macromol.5b02642
Macromolecules 2016, 49, 2646−2655

accompanied by relatively large absolute values of the loss modulus $G''(T)$. Both findings can be interpreted as an indication for the occurrence of interfacial material with intermediate softening temperatures containing isoprene and BF units. The fraction of interfacial material increased obviously with increasing PBF content as indicated by larger G'' contributions. Interestingly, an additional very broad, smeared relaxation process with a maximum near 30 °C was indicated for samples with higher PBF contents (FIF-22, FIF-31). This finding may be related to the existence of a relative uniform interphase with given isoprene-BF contents apart from the pure PI and PBF phases.

Stress−Strain Behavior of FIF Triblock Copolymers. After studying the softening behavior, the tensile strength of FIF triblock copolymers was tested. It was found that the Young's modulus (E), tensile stress (σ), and strain at break (ε_B) could be tuned based on the volume fraction of PBF (Table 4). The rather low Young's modulus for FIF-10 and FIF-14 gave indications for a noncontinuous hard phase in the rubbery matrix. Specifically, FIF-14 displayed highest strain at break of 1394 ± 66% and the best tensile strength of 14.3 ± 1.3 MPa (Figure 7) among all samples. These tensile properties were competitive with Kraton D1112P, a commercial SIS triblock copolymer used in sealants, coating, adhesives, and other elastomer modification. (For Kraton D1112P, the ultimate tensile strength is 10.3 MPa and the strain at break is 1400%.[30]) Typical TPE behavior of FIF-14 with efficient physical cross-linking was thus demonstrated.

Three types of failure characteristics were observed for the FIF-polymers: (i) FIF-10 showed an elastomeric behavior at the beginning but no strain hardening is found. This gave rise to the assumption that the physical cross-links were less effective here: there was no sufficient interaction between the PBF-blocks within the domains so that PBF-blocks were pulled out easily. Chain pullout in SIS block copolymers is discussed e.g. by Baeurle.[44] (ii) For FIF-14 a strain hardening region was clearly observed indicating that pull-out of PBF-blocks was more effectively hindered by their higher molecular weight. This resulted in a stronger cross-linked network in FIF-14 (Table 4) in comparison to FIF-10. However, at high strains, deviations between model and experimental data were observed for FIF-14, indicating that physical cross-links became weak (pullout of PBF-blocks from existing domains and partly re-formation of new, smaller domains), resulting in plastic deformation (Figure 8). (iii) FIF-22 and FIF-31 exhibited thermoplastic behavior with higher Young's modulus and much lower strain at break, leaving the assumption that a continuous hard phase was formed. Further evidence for this assumption was the appearance of a yield point for FIF-31 at 3.5% strain and 5.3 MPa.

The parameters of the nonaffine tube model for FIF-10 and FIF-14 are shown in Table 4. For the tube model parameters G_c and G_e, an increase was noticed when changing the PBF content from 10 to 14 vol %; i.e., the total cross-link density increases. The absolute increase was slightly more pronounced for G_e. The effect in G_e was probably caused by the higher molecular weight of the PI-spacer in FIF-14 (Table 3), since more entanglements can form. The increase in G_c may be assigned to the stronger retaining force of longer end blocks in the domains. The SAXS data in Table 5 revealed that the average PBF−PI domain distance $d_{AV,\ PBF-PI}$ was similar for FIF-10 and FIF-14 although the PBF content has been changed. Hence, one could argue that the number of the spherical domains cannot rise significantly if only their diameter increases. Moving from weak to improved cross-linking, G_c would be expected to remain approximately constant while the upturn was better captured by the rubber elasticity model. Consequently, lower n values are obtained, which was due to the fact that entanglement trapping only works efficiently if PBF block pull out was hindered. This trend can be seen in Table 4.

Microphase Separation Behavior. The microphase separation behavior between PBF and PI in FIF triblock copolymers was investigated by SAXS. In the SAXS measurements (Figure 9a), microphase separation without long-range order was observed between PBF and PI in all FIF samples. A broad secondary peak was observed approximately at $3.3q^*$ after the maximum primary peak q^*. However, none of the reflection pattern (q/q^*) of FIF-10, -14, -22, and -31 matched with Bragg reflection for the morphology of any A−B−A type block copolymer.[45] The broad, rounded peaks separated by cusp-like minima in the SAX data are characteristic of form factor scattering resulting from the shape of the microphase separated domains. The absence of Bragg peaks indicates that these domains are not ordered on a lattice, but rather are randomly distributed.[46] Both spherical and cylinder form factor can be used to fit SAXS data of FIF-10 and FIF-14 (Figure 9b). This indicates a morphology of disordered, worm-like, microphase-separated spheres and cylinders in FIF-10 and FIF-14. For FIF-22 and FIF-31 SAXS data can be fit to cylindrical form factors with radii ranging from 9 to 16 nm for the various samples. This indicates a morphology of disordered, worm-like, microphase-separated cylinders for FIF-22 and FIF-31. Since all samples were annealed at 155 °C for 12 h in order to prevent thermo-cross-linking of unsaturated carbon−carbon double bond in FIFs, this annealing condition might be insufficient for glassy PBF domains to reorganize into an ordered lattice.

The average PBF−PI domain distance ($d_{AV,\ PBF-PI}$) of all four FIF samples were calculated from $d_{AV,PBF-PI} = 2\pi/q^*$ and summarized in Table 5. As the volume fraction of PBF (ϕ_{PBF}) increased from 9.5% to 30.9%, the average PBF−PI domain distance increased from 35.3 to 57.1 nm. Assuming PBF in FIF-10 and FIF-14 formed spherical assemblies, the average diameter of the PBF spheres, $d_{AV,PBF,sph}$, can be calculated by eq 3:[47]

$$d_{AV,PBF,sph} = d_{AV,PBF-PI}\sqrt[3]{\frac{3}{\pi}\phi_{PBF}} \tag{3}$$

Lastly, bulk morphology of FIF-10 was examined by atomic force microscopy using tapping-mode in the air on a cryo-microtomed cross section (Figure 10). Disordered worm-like domains were observed in the phase image (Figure 10b), since the observed contrast in the phase images mostly reflects differences in elastic and adhesive properties between PI and PBF blocks. The length scales and periodicities from AFM measurement were consistent with those from SAXS.

CONCLUSIONS

In summary, FIF triblock copolymers with four different compositions were synthesized by living anionic polymerization in benzene at room temperature. Dynamic mechanical analysis indicated that the softening temperature of PBF in FIF copolymers was around 145 °C. Tensile testing of sample FIF-14 (with 14 vol % of PBF) displayed a maximum stress of

DOI: 10.1021/acs.macromol.5b02642
Macromolecules 2016, 49, 2646−2655

14.3 ± 1.3 MPa with strain at break of 1394 ± 66%. SAXS profile showed microphase separation of PBF and PI without long-range order. Atomic force microscopy (AFM) in tapping mode revealed a disordered worm-like morphology of FIF-10. The different types of additives used for anionic polymerization have a significant effect on the T_g of PBF homopolymer. Among the additives studied, the initiation system of DME/*n*-BuLi produced PBF with the highest T_g, above 190 °C.

■ ASSOCIATED CONTENT

Supporting Information

The Supporting Information is available free of charge on the ACS Publications website at DOI: 10.1021/acs.macromol.5b02642.

Figures S1−S4 (PDF)

■ AUTHOR INFORMATION

Corresponding Authors

*E-mail nkang1@utk.edu (N.-G.K).
*E-mail jimmy@utk.edu (J.M.).

Notes

The authors declare no competing financial interest.

■ ACKNOWLEDGMENTS

We are grateful for financial support from the U.S. National Science Foundation, Award 1237787 from the NSF Partnerships for Innovation, Building Innovation Capacity program. This work also was supported by the Bill & Melinda Gates Foundation through their Grand Challenges Explorations program. We also acknowledge partial support from the Army Research Office under Contract W911-NF-11-0417. The authors thank M. Menzel and J. Klehm for support with the AFM images.

■ REFERENCES

(1) (a) Szwarc, M. *Nature* **1956**, *178*, 1168. (b) Szwarc, M.; Levy, M.; Milkovich, R. *J. Am. Chem. Soc.* **1956**, *78*, 2656.
(2) Hadjichristidis, N.; Pitsikalis, M.; Pispas, S.; Iatrou, H. *Chem. Rev.* **2001**, *101*, 3747.
(3) Hirao, A.; Goseki, R.; Ishizone, T. *Macromolecules* **2014**, *47*, 1883.
(4) Hsieh, H.; Quirk, R. P. *Anionic Polymerization: Principles and Practical Applications*; Marcel Dekker Inc.: New York, 1996.
(5) Quirk, R. P. *Applications of Anionic Polymerization Research*; Oxford University Press: Washington, DC, 1998.
(6) Holden, G. *Thermoplastic Elastomers*; Hanser-Gardner Publications: New York, 1996.
(7) Holden, G.; Milkovich, R. U.S. Patent 3265765 A, 1966.
(8) Handlin, D. L.; Trenor, S.; Wright, K. Applications of Thermoplastic Elastomers Based on Styrenic Block Copolymers. In *Macromolecular Engineering: Precise Synthesis, Materials Properties, Applications*; Matyjaszewski, K., Gnanou, Y., Leibler, L., Eds.; Wiley-VCH: 2007; Vol. 4, pp 2001−2031.
(9) Fetters, L. J.; Morton, M. *Macromolecules* **1969**, *2*, 453.
(10) Bolton, J. M.; Hillmyer, M. A.; Hoye, T. R. *ACS Macro Lett.* **2014**, *3*, 717.
(11) Fetters, L. J.; Firer, E. M.; Dafauti, M. *Macromolecules* **1977**, *10*, 1200.
(12) Kobayashi, S.; Kataoka, H.; Ishizone, T.; Kato, T.; Ono, T.; Kobukata, S.; Ogi, H. *Macromolecules* **2008**, *41*, 5502.
(13) Alfonzo, C. G.; Fleury, G.; Chaffin, K. A.; Bates, F. S. *Macromolecules* **2010**, *43*, 5295.
(14) Hucul, D. A.; Hahn, S. F. *Adv. Mater.* **2000**, *12*, 1855.
(15) Yu, Y.; Dubois, P.; Teyssié, P.; Jérôme, R. *Macromolecules* **1997**, *30*, 4254.
(16) Yu, J. M.; Dubois, P.; Jérôme, R. *Macromolecules* **1997**, *30*, 6536.
(17) Yu, J. M.; Dubois, P.; Jérôme, R. *Macromolecules* **1996**, *29*, 8362.
(18) Yu, J. M.; Dubois, P.; Jérôme, R. *Macromolecules* **1996**, *29*, 7316.
(19) Fodor, Z.; Kennedy, J. P. *Polym. Bull.* **1992**, *29*, 697.
(20) Puskas, J. E.; Kaszas, G.; Kennedy, J. P.; Hager, W. G. *J. Polym. Sci., Part A: Polym. Chem.* **1992**, *30*, 41.
(21) Li, D.; Faust, R. *Macromolecules* **1995**, *28*, 4893.
(22) Kennedy, J. P.; Puskas, J. E.; Kaszas, G.; Hager, W. G. U.S. Patent 4946899 A, 1990.
(23) Imaeda, T.; Hashimoto, T.; Irie, S.; Urushisaki, M.; Sakaguchi, T. *J. Polym. Sci., Part A: Polym. Chem.* **2013**, *51*, 1796.
(24) Mosnáček, J.; Yoon, J. A.; Juhari, A.; Koynov, K.; Matyjaszewski, K. *Polymer* **2009**, *50*, 2087.
(25) Juhari, A.; Mosnáček, J.; Yoon, J. A.; Nese, A.; Koynov, K.; Kowalewski, T.; Matyjaszewski, K. *Polymer* **2010**, *51*, 4806.
(26) Kosaka, Y.; Kitazawa, K.; Inomata, S.; Ishizone, T. *ACS Macro Lett.* **2013**, *2*, 164.
(27) Kosaka, Y.; Goseki, R.; Kawauchi, S.; Ishizone, T. *Macromol. Symp.* **2015**, *350*, 55.
(28) Kosaka, Y.; Kawauchi, S.; Goseki, R.; Ishizone, T. *Macromolecules* **2015**, *48*, 4421.
(29) Londergan, T. M.; Teng, C. J.; Weber, W. P. *Macromolecules* **1999**, *32*, 1111.
(30) Material Property Data: Kraton D1112P (SIS) Linear Block Copolymer; http://www.matweb.com/search/datasheet.aspx?matguid=ec777ddb6a3540ae977fb8f9a53c4d64.
(31) Cunningham, R. E.; Auerbach, M.; Floyd, W. J. *J. Appl. Polym. Sci.* **1972**, *16*, 163−173.
(32) Uhrig, D.; Mays, J. W. *J. Polym. Sci., Part A: Polym. Chem.* **2005**, *43*, 6179.
(33) Klüppel, M.; Schramm, J. *Macromol. Theory Simul.* **2000**, *9*, 742.
(34) Heinrich, G.; Klüppel, M.; Vilgis, T. A. *Curr. Opin. Solid State Mater. Sci.* **2002**, *6*, 195.
(35) (a) Domurath, J.; Saphiannikova, M.; Ausias, G.; Heinrich, G. *J. Non-Newtonian Fluid Mech.* **2012**, *171−172*, 8−16. (b) Schlegel, R.; Duan, Y. X.; Weidisch, R.; Hölzer, S.; Schneider, K.; Stamm, M.; Uhrig, D.; Mays, J. W.; Heinrich, G.; Hadjichristidis, N. *Macromolecules* **2011**, *44*, 9374.
(36) Hsieh, H.; Quirk, R. P. *Anionic Polymerization: Principles and Practical Applications*; Marcel Dekker Inc.: New York, 1996; Chapter 9, pp 197−235.
(37) Natori, I.; Inoue, S. *Macromolecules* **1998**, *31*, 4687.
(38) Hong, K.; Mays, J. W. *Macromolecules* **2001**, *34*, 782.
(39) Halasa, A. F.; Lohr, D. F.; Hall, J. E. *J. Polym. Sci., Polym. Chem. Ed.* **1981**, *19*, 1357.
(40) Poshyachinda, S.; Edwards, H. G. M.; Johnson, A. F. *Polymer* **1997**, *38*, 535.
(41) Uhrig, D.; Hong, K.; Mays, J. W.; Kilbey, S. M.; Britt, P. F. *Macromolecules* **2008**, *41*, 9480.
(42) Chadwick, S. T.; Rennels, R. A.; Rutherford, J. L.; Collum, D. B. *J. Am. Chem. Soc.* **2000**, *122*, 8640.
(43) Iatrou, H.; Mays, J. W.; Hadjichristidis, N. *Macromolecules* **1998**, *31*, 6697.
(44) Baeurle, S. A.; Hotta, A.; Gusev, A. A. *Polymer* **2005**, *46*, 4344.
(45) Skoulios, A. E. In *Developments on Block Copolymers-1*; Applied Science Publishers: New York, 1982.
(46) Beyer, F. L.; Gido, S. P.; Büschl, C.; Iatrou, H.; Uhrig, D.; Mays, J. W.; Chang, M. Y.; Garetz, B. A.; Balsara, N. P.; Tan, N. B.; Hadjichristidis, N. *Macromolecules* **2000**, *33*, 2039.
(47) Schlegel, R.; Duan, Y. X.; Weidisch, R.; Hölzer, S.; Schneider, K.; Stamm, M.; Uhrig, D.; Mays, J. W.; Heinrich, G.; Hadjichristidis, N. *Macromolecules* **2011**, *44*, 9374.

DOI: 10.1021/acs.macromol.5b02642
Macromolecules 2016, 49, 2646−2655